International Journal of the Physical Sciences Vol. 6(11), pp. 2681-2696, 4 June, 2011
Available online at http://www.academicjournals.org/IJPS
DOI: 10.5897/IJPS11.493
ISSN 1992 - 1950 ©2011 Academic Journals

Full Length Research Paper

Vibration and stability of multi-cracked beams under compressive axial loading

Murat Kisa

Department of Mechanical Engineering, Faculty of Engineering, Harran University, Sanliurfa-Turkey. E-mail: mkisa@harran.edu.tr Tel: +905334524865. Fax: +904143183799.

Accepted 18 May, 2011

In this study, a novel technique for the vibration and stability analyses of axially loaded beams with multi-cracks was offered. In the model which combines the finite element and component mode synthesis methods, the cracks were modelled as massless springs. Initially, stability analysis was completed and then three numerical cases were given to explore the effects of axial load levels, crack locations and ratios on the natural frequencies and mode shapes of the beams. Very good conformities between outcomes of the current study and those in literature, gave the confidence that the proposed method which could be used to predict crack positions, crack sizes and critical buckling load of defected structures by using the modal data, was reliable and effective.

Key words: Finite element analysis, damage, failure assessment, pressurised components.

INTRODUCTION

Any changes in the mass and stiffness of a member result in alterations in its dynamic and static behaviours. Cracks in a structural element modify its stiffness and damping properties. In view of that, the modal data of the structure contain information relating to the position and size of the deficit. Structural defects are source of local flexibilities and cause deficiencies in structural resistance. Structures quite often are operated under axial loading. For that reason, in addition to crack ratios and locations, influence of applied load on the dynamical characteristics should also be searched. Working conditions, environment, mechanical vibrations, long-term service or applied cyclic loads may result in the initiation of structural defects such as cracks in the structures. Accordingly, the determination of the effects of these deficiencies on the vibration safety and stability of the structures forms an important aspect of investigation. The effects of the cracks on the dynamical behaviour of the structures have been investigated by many researchers in the past (Cawley and Adams, 1979; Gounaris and Dimarogonas, 1988; Shen and Chu, 1992; Krawczuk and Ostachowicz, 1993; Ruotolo et al., 1996; Kisa et al., 1998; Shifrin and Ruotolo, 1999; Kisa and Brandon, 2000a, b; Viola et al., 2001; Krawczuk, 2002; Patil and Maiti, 2003; Kisa, 2004).

Relatively few researchers have studied the effects of axial load on the vibration and stability behaviour of cracked beams. Takahashi (1998) analysed the vibration and stability of a non-uniform cracked shaft subjected to a tangential follower force by using the transfer matrix method. Li (2001) investigated buckling of multi-step cracked columns with shear deformation. He presented an approach that combines the exact buckling solution of a one-step column and the transfer matrix method for solving the entire and partial buckling of a multi-step column with various end conditions, with or without cracks and shear deformation, subjected to concentrated axial loads. Li (2003) presented the exact solutions for buckling of multi-step non-uniform columns with cracks subjected to concentrated and distributed axial loads. A model of massless rotational spring was adopted to describe the local flexibility induced by cracks in the column. Lee et al. (2002) explored the free vibration analysis of axially compressed laminated composite beam-columns with multiple delaminations. They obtained the characteristic equation of multi-delaminated beam-column by dividing the global multi-delaminated beam-columns into segments and by imposing recurrence relation from the continuity conditions on each sub-beam-column.

Zheng and Fan (2003) studied the vibration and stability of cracked hollow-sectional beams. Wang (2004) presented a comprehensive analysis of the stability of a cracked beam subjected to a follower compressive load and obtained buckling load of the cracked beam through dynamic analysis of the beam. Hsu (2005), by using the differential quadrature method (DQM), numerically formulated the eigenvalue problems of clamped-free and hinged-hinged Bernoulli-Euler cracked beams on elastic foundation with axial force. Binici (2005) investigated the vibration of beams with multiple open cracks subjected to axial force. His method uses one set of end conditions as initial parameters for determining the mode shape functions. Mei et al. (2006) presented wave vibration analysis of an axially loaded cracked beam considering the effects of shear deformation and rotary inertia. Gurel (2007) studied the buckling of slender prismatic circular cross-sectional columns with multiple non-propagating edge cracks. Arbodela-Monsalve et al. (2007) investigated the stability and free vibration analyses of a Timoshenko beam-column with generalised end conditions subjected to constant axial load and weakened by a cracked section along its span. They included the detrimental effects of a single weakened section and the beneficial effects of a lateral bracing located at the discontinuity. Viola et al. (2007) studied the free vibration of axially loaded cracked Timoshenko beam structures. They introduced a new procedure based on the coupling of dynamic stiffness matrix and line-spring element to model the cracked beam. Aristizabal-Ochoa (2007) offered a model to analyse the static and dynamic stability of uniform shear beam-columns under generalised boundary conditions. This model includes the combined effects of shear deformations, an axially applied load linearly distributed along beam span, the translational and rotational inertias of the member's mass and of the rotational and translational lumped masses located at the ends of the member. Yang et al. (2008), by employing the modal series expansion technique, presented an analytical method to investigate the free and forced vibration of cracked inhomogeneous Euler-Bernoulli beams under an axial force and a moving load. A simple and proficient analytical approach to determine the vibratory characteristics of axially loaded Timoshenko and Euler-Bernoulli beams with arbitrary number of cracks is proposed by Aydin (2007, 2008). In the study, the local compliance induced by a crack was described by a massless rotational spring and a set of boundary conditions were used as initial parameters to define the mode shapes of the segment of the beam before the first crack. Kukla (2009) investigated the free vibration and stability of stepped columns with cracks. The cracks in the column were modelled by massless rotational springs and the frequency equation was obtained by using the Green's functions. Caddemi and Calio (2009) presented the closed-form expressions for the vibration modes of the Euler–Bernoulli beam in the presence of multiple concentrated cracks modelled as a sequence of Dirac's delta generalised functions in the flexural stiffness. They conducted a parametric analysis for different boundary conditions in order to investigate the influence of the number, position, and intensity of the cracks on the dynamical properties of the Euler–Bernoulli beam. Recently, Bilgehan (2011) presented an adaptive neuro-fuzzy inference system (ANFIS) and artificial neural network (ANN) model and successfully applied for the buckling analysis of slender prismatic columns with a single non-propagating open edge crack subjected to axial loads.

Hurty (1965) proposed a method known as component mode synthesis or substructure technique which enabled the problem to be broken up into separate elements and thus considerably reduced its complexity. In the present study, vibration and stability analyses of multi-cracked beams subjected to axial loads are explored utilising the component mode and finite element methods. Offered method detaches a non-linear problem into linear components from the crack sections. Consequently, the initial non-linear system with local discontinuities in stiffness at the crack sections is now composed of a number of linear segments. Substructures are connected by artificial and massless springs whose stiffness coefficients are functions of the compliance coefficients. The offered method in the current study is believed to be applied for the first time to the axially loaded beams with multi-cracks.

MATHEMATICAL FORMULATION OF THE MODEL

The model studied in the current study is an axially loaded beam with uniform cross section of A and multiple open edge cracks of depths r_i at variable locations L_i (Figure 1). The beam has m-1 cracks; therefore it is separated into m components from the crack sections which lead to a substructure formula. In view of that, as aforementioned, the global non-linear system with local stiffness discontinuities is separated into m linear subsystems. Every component is also broken up into finite elements z_i with two nodes and three degrees of freedom at the each node as displayed in Figure 2.

Evaluation of flexibility matrix induced by a crack

Deficiencies such as cracks in structures are sources of local flexibilities which affect the dynamic and static behaviours of the structures. Flexibility coefficients can be expressed by stress intensity factors derived through Castigliano's theorem in the linear elastic range. The strain energy release rate, J, represents the elastic energy in relation to a unit increase in length ahead of

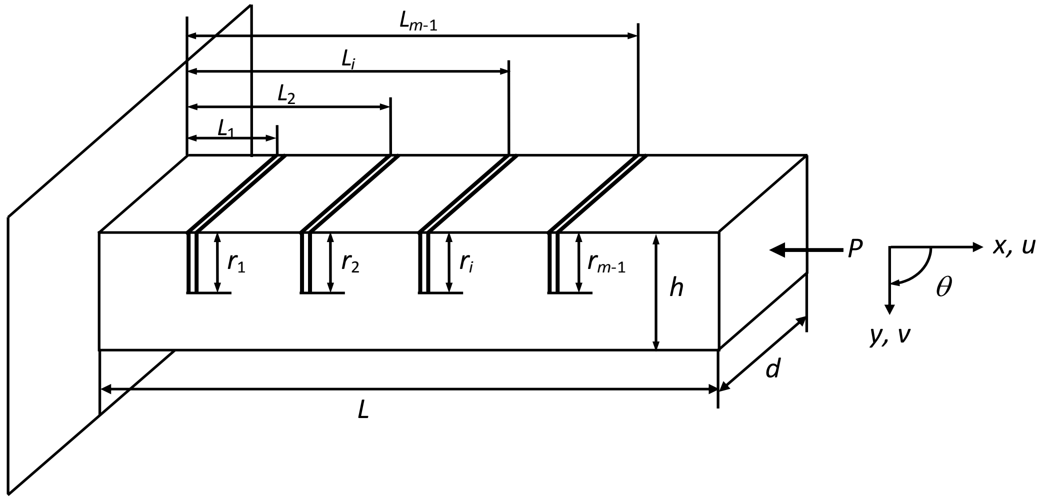

Figure 1. An axially loaded multi-cracked cantilever beam.

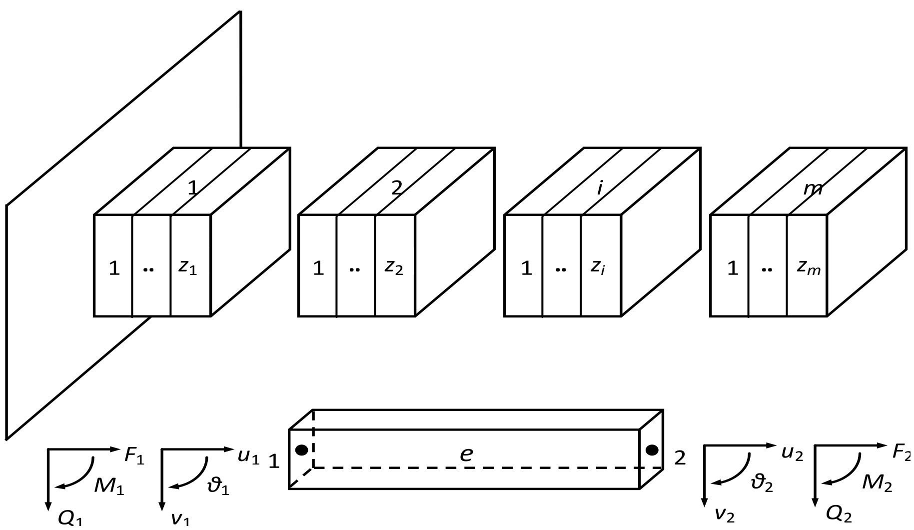

Figure 2. Finite element model of multi-cracked beam.

the crack front. For plane strain, J can be given as (Irwin, 1960)

$$J = \frac{1-\nu^2}{E} K_I{}^2 + \frac{1-\nu^2}{E} K_{II}{}^2 + \frac{1+\nu}{E} K_{III}{}^2 \tag{1}$$

Where; K_I, K_{II}, K_{III}, ν and E are the stress intensity factors for the modes *I*, *II, III* deformation types, Poisson's ratio and modulus of elasticity, respectively. Let U be the strain energy of a cracked structure with a crack area A under the nodal loads P_i ($P_1 = F$, $P_2=Q$, $P_3 = M$) then the relation between J and U is

$$J = \frac{\partial U(P_i, A)}{\partial A} \tag{2}$$

In accordance with the Castigliano's theorem, the additional displacement caused by the crack in the direction of P_i can be given as:

$$u_i = \frac{\partial U(P_i, A)}{\partial P_i} \tag{3}$$

Substituting Equation 2 into 3 gives the final expression between displacement and strain energy release rate J as:

$$u_i = \frac{\partial}{\partial P_i} \int_A J(P_i, A)\, dA \tag{4}$$

Now the flexibility coefficients which are the functions of the crack shape and stress intensity factors can be introduced as follows:

$$c_{ij} = \frac{\partial u_i}{\partial P_j} = \frac{\partial^2}{\partial P_i \partial P_j} \int_A J(P_i, A) dA \tag{5}$$

The flexibility coefficients c_{ij} are found from the fracture mechanics method proposed by Dimarogonas and Paipetis (1983). Dimensionless flexibility coefficients are calculated numerically. Since the shear force does not contribute to the opening mode of the crack, the flexibility matrix, in relation to displacements (u, v, θ), can be written as:

$$C = \begin{bmatrix} c_{11} & 0 & c_{13} \\ 0 & c_{22} & 0 \\ c_{31} & 0 & c_{33} \end{bmatrix}_{(3x3)} \tag{6}$$

Using the flexibility matrix, the stiffness matrix generated by a crack is given as:

$$K_{cr} = \begin{bmatrix} C^{-1} & -C^{-1} \\ -C^{-1} & C^{-1} \end{bmatrix}_{(6x6)} \tag{7}$$

Component mode analysis

Consider an axially loaded component i, whose equation of motion in matrix notation can be given as follows:

$$M_i \ddot{q}_i + D_i \dot{q}_i + K_i q_i + P K_{Gi} q_i = f_i(t) \tag{8}$$

Where; P, q_i, $f_i(t)$, M_i, D_i, K_i and K_{Gi} are the applied compressive load, generalised displacement vector, external force vector, mass, damping, stiffness and geometric stiffness matrices, respectively, for the component i. Mass and stiffness matrices are taken from the work of Friedman and Kosmatka (1993). For an element i with the length of L, geometric stiffness matrix can be given as follows:

$$[K_{Gi}] = \frac{1}{L} \begin{bmatrix} 0 & 0 & 0 & 0 & 0 & 0 \\ 0 & \frac{6}{5} & \frac{L}{10} & 0 & -\frac{6}{5} & \frac{L}{10} \\ 0 & \frac{L}{10} & \frac{2}{15}L^2 & 0 & -\frac{L}{10} & -\frac{L^2}{30} \\ 0 & 0 & 0 & 0 & 0 & 0 \\ 0 & -\frac{6}{5} & -\frac{L}{10} & 0 & \frac{6}{5} & -\frac{L}{10} \\ 0 & \frac{L}{10} & -\frac{L^2}{30} & 0 & -\frac{L}{10} & \frac{2}{15}L^2 \end{bmatrix} \tag{9}$$

For undamped free vibration analysis, Equation 8 rewritten as:

$$M_i \ddot{q}_i + (K_i + P K_{Gi}) q_i = 0 \tag{10}$$

Assuming that

$$\{q_i\} = \{\varphi\} \sin(\omega t + \beta), \quad \{\ddot{q}_i\} = -\omega^2 \{\varphi\} \sin(\omega t + \beta) \tag{11}$$

and substituting them into Equation 10, the standard free vibration equation for the component i is obtained as,

$$\omega^2 M_i \varphi = (K_i + P K_{Gi}) \varphi \tag{12}$$

which gives eigenvalues $\omega^2_{i1}, ..., \omega^2_{in}$ and modal matrix φ_i for the component i. q_i can be defined as principal coordinate vector p_i by using the following relation

$$q_i = \varphi_i p_i \tag{13}$$

Premultiplying Equation 13 by φ_i^T and substituting it into Equation 10 gives the following equation.

$$(\varphi_i^T M_i \varphi_i) \ddot{p}_i + (\varphi_i^T (K_i + P K_{Gi}) \varphi_i) p_i = 0 \tag{14}$$

where

$$\begin{aligned} \varphi_i^T M_i \varphi_i &= [m_m] \\ \varphi_i^T (K_i + P K_{Gi}) \varphi_i &= [k_m] \end{aligned} \tag{15}$$

Where: $[m_m]$ and $[k_m]$ are the modal mass and stiffness matrices, respectively. If the modal matrix is normalised by the mass, mass normalised mode vector ψ_{ij} can be given as:

$$\psi_{ij} = \frac{\varphi_{ij}}{\sqrt{m_{jj}}} \tag{16}$$

q_i can be defined as principal coordinate vector s_i by using the following transformation

$$q_i = \psi_i s_i \tag{17}$$

Premultiplying Equation 17 by ψ_i^T and substituting it into Equation 10 results in

$$(\psi_i^T M_i \psi_i) \ddot{s}_i + (\psi_i^T (K_i + P K_{Gi}) \psi_i) s_i = 0 \tag{18}$$

Where:

$$\begin{aligned} (\psi_i^T M_i \psi_i) &= I \\ (\psi_i^T (K_i + P K_{Gi}) \psi_i) &= \omega_i^2 \end{aligned} \tag{19}$$

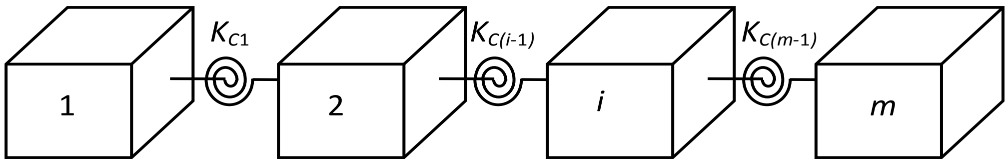

Figure 3. Joining of components with springs.

Using Equation 19, Equation 18 becomes

$$I\,\ddot{s}_i + \omega_i^2\, s_i = 0 \tag{20}$$

Where: ω_i^2 is a diagonal matrix comprising the eigenvalues of component i.

Combination process of the components

Consider components i (i = 1, 2,..., m) which are undamped and supposed to be linked together by means of springs capable of carrying axial, shearing and bending effects, as illustrated in Figure 3. Kinetic (T) and strain (U) energies of components, in terms of principal modal coordinates, can be given as:

$$T=\frac{1}{2}\begin{Bmatrix}\dot{s}_1\\ \dot{s}_2\\ \dots\\ \dot{s}_m\end{Bmatrix}^T\left(\begin{bmatrix}\psi_1&0&\dots&0\\0&\psi_2&\dots&0\\\dots&\dots&\dots&\dots\\0&0&\dots&\psi_m\end{bmatrix}^T\begin{bmatrix}M_1&0&\dots&0\\0&M_2&\dots&0\\\dots&\dots&\dots&\dots\\0&0&\dots&M_m\end{bmatrix}\begin{bmatrix}\psi_1&0&\dots&0\\0&\psi_2&\dots&0\\\dots&\dots&\dots&\dots\\0&0&\dots&\psi_m\end{bmatrix}\right)\begin{Bmatrix}\dot{s}_1\\ \dot{s}_2\\ \dots\\ \dot{s}_m\end{Bmatrix} \tag{21}$$

$$U=\frac{1}{2}\begin{Bmatrix}s_1\\ s_2\\ \dots\\ s_m\end{Bmatrix}^T\left(\begin{bmatrix}\psi_1&0&\dots&0\\0&\psi_2&\dots&0\\\dots&\dots&\dots&\dots\\0&0&\dots&\psi_m\end{bmatrix}^T\begin{bmatrix}(K+PK_G)_1&0&\dots&0\\0&(K+PK_G)_2&\dots&0\\\dots&\dots&\dots&\dots\\0&0&\dots&(K+PK_G)_m\end{bmatrix}\begin{bmatrix}\psi_1&0&\dots&0\\0&\psi_2&\dots&0\\\dots&\dots&\dots&\dots\\0&0&\dots&\psi_m\end{bmatrix}\right)\begin{Bmatrix}s_1\\ s_2\\ \dots\\ s_m\end{Bmatrix}$$

Where:

$$\begin{bmatrix}\psi_1&0&\dots&0\\0&\psi_2&\dots&0\\\dots&\dots&\dots&\dots\\0&0&\dots&\psi_m\end{bmatrix}^T\begin{bmatrix}M_1&0&\dots&0\\0&M_2&\dots&0\\\dots&\dots&\dots&\dots\\0&0&\dots&M_m\end{bmatrix}\begin{bmatrix}\psi_1&0&\dots&0\\0&\psi_2&\dots&0\\\dots&\dots&\dots&\dots\\0&0&\dots&\psi_m\end{bmatrix}=\begin{bmatrix}I&0&\dots&0\\0&I&\dots&0\\\dots&\dots&\dots&\dots\\0&0&\dots&I\end{bmatrix} \tag{22}$$

$$\begin{bmatrix}\psi_1&0&\dots&0\\0&\psi_2&\dots&0\\\dots&\dots&\dots&\dots\\0&0&\dots&\psi_m\end{bmatrix}^T\begin{bmatrix}(K+PK_G)_1&0&\dots&0\\0&(K+PK_G)_2&\dots&0\\\dots&\dots&\dots&\dots\\0&0&\dots&(K+PK_G)_m\end{bmatrix}\begin{bmatrix}\psi_1&0&\dots&0\\0&\psi_2&\dots&0\\\dots&\dots&\dots&\dots\\0&0&\dots&\psi_m\end{bmatrix}=\begin{bmatrix}\omega_1^2&0&\dots&0\\0&\omega_2^2&\dots&0\\\dots&\dots&\dots&\dots\\0&0&\dots&\omega_m^2\end{bmatrix}$$

The strain energy of the connectors, in terms of principal modal coordinates, is

$$U_C=\frac{1}{2}\begin{Bmatrix}s_1\\ s_2\\ \dots\\ s_m\end{Bmatrix}^T\left(\begin{bmatrix}\psi_1&0&\dots&0\\0&\psi_2&\dots&0\\\dots&\dots&\dots&\dots\\0&0&\dots&\psi_m\end{bmatrix}^T K_C\begin{bmatrix}\psi_1&0&\dots&0\\0&\psi_2&\dots&0\\\dots&\dots&\dots&\dots\\0&0&\dots&\psi_m\end{bmatrix}\right)\begin{Bmatrix}s_1\\ s_2\\ \dots\\ s_m\end{Bmatrix} \tag{23}$$

Where: K_C is the connection matrix comprising the cracked nodal elements' stiffness matrices and can be given as:

$$K_C=\begin{bmatrix}K_{cr,1}&0&\dots&0\\0&K_{cr,2}&\dots&0\\\dots&\dots&\dots&\dots\\0&0&\dots&K_{cr,m-1}\end{bmatrix} \tag{24}$$

The total strain energy of the system is

$$U_T=\frac{1}{2}\begin{Bmatrix}s_1\\ s_2\\ \dots\\ s_m\end{Bmatrix}^T\left(\begin{bmatrix}\psi_1&0&\dots&0\\0&\psi_2&\dots&0\\\dots&\dots&\dots&\dots\\0&0&\dots&\psi_m\end{bmatrix}^T\begin{bmatrix}(K+PK_G)_1&0&\dots&0\\0&(K+PK_G)_2&\dots&0\\\dots&\dots&\dots&\dots\\0&0&\dots&(K+PK_G)_m\end{bmatrix}\begin{bmatrix}\psi_1&0&\dots&0\\0&\psi_2&\dots&0\\\dots&\dots&\dots&\dots\\0&0&\dots&\psi_m\end{bmatrix}+\begin{bmatrix}\psi_1&0&\dots&0\\0&\psi_2&\dots&0\\\dots&\dots&\dots&\dots\\0&0&\dots&\psi_m\end{bmatrix}^T K_C\begin{bmatrix}\psi_1&0&\dots&0\\0&\psi_2&\dots&0\\\dots&\dots&\dots&\dots\\0&0&\dots&\psi_m\end{bmatrix}\right)\begin{Bmatrix}s_1\\ s_2\\ \dots\\ s_m\end{Bmatrix} \tag{25}$$

Using Lagrange's equation with Equations 21 to 25, the eigenvalue equation can be given as:

$$\left(\begin{bmatrix}\omega_1^2&0&\dots&0\\0&\omega_2^2&\dots&0\\\dots&\dots&\dots&\dots\\0&0&\dots&\omega_m^2\end{bmatrix}+\begin{bmatrix}\psi_1&0&\dots&0\\0&\psi_2&\dots&0\\\dots&\dots&\dots&\dots\\0&0&\dots&\psi_m\end{bmatrix}^T K_C\begin{bmatrix}\psi_1&0&\dots&0\\0&\psi_2&\dots&0\\\dots&\dots&\dots&\dots\\0&0&\dots&\psi_m\end{bmatrix}-\omega^2\begin{bmatrix}I&0&\dots&0\\0&I&\dots&0\\\dots&\dots&\dots&\dots\\0&0&\dots&I\end{bmatrix}\right)\begin{Bmatrix}s_1\\ s_2\\ \dots\\ s_m\end{Bmatrix}=\begin{Bmatrix}0\\ 0\\ \dots\\ 0\end{Bmatrix} \tag{26}$$

Utilising the Equation 26, modal data of the multi-cracked beam can be determined. The displacements for each component are then calculated by Equation 17.

Buckling analysis

For the free vibration analysis of the axially loaded cracked beams, a compressive axial load is applied to the cracked beam. The magnitude of the applied axial load should not exceed the critical buckling load and as a consequence before the free vibration analysis, initially a buckling analysis of the cracked beam is carried out to obtain the critical buckling loads. As previously given, the equation of motion for the free vibration of an axially loaded cracked beam can be given, in matrix notation as:

$$M\,\ddot{q}+(K+K_C+P\,K_G)q=0 \tag{27}$$

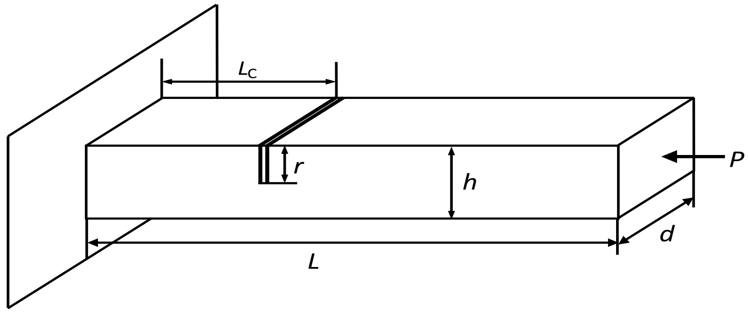

Figure 4. A fixed-free axially loaded cracked beam.

In the static case ($\ddot{q}=0$) Equation 27 gives the typical buckling equation

$$(K+K_C+PK_G)q=0 \quad (28)$$

For a non-trivial solution, one can write

$$\left|(K+Kc)+\lambda K_G\right|=0 \quad (29)$$

This is a well known eigenvalue problem and the smallest value of λ gives the primary critical buckling load (P_{cr}) for the cracked beam.

CASE STUDIES

Axially loaded fixed-free beam with a crack

First sample is chosen as a fixed-free beam with a crack under compressive axial load (Figure 4) to confirm the reliability and correctness of the offered procedure. The geometrical and material properties of the beam are chosen as; length L = 3 m, height h = 0.2 m, width d = 0.2 m and Young's modulus E = 216x10^9 N m^{-2}, Poisson's ratio ν = 0.33, material density ρ = 7.85x10^3 kgm^{-3}, respectively. Previous to vibration investigation, a buckling analysis is done to find the critical buckling loads.

Buckling analysis of fixed-free beam with a crack

Euler formula gives the fundamental critical buckling load of the fixed-free intact beam as:

$$P_e=\frac{\pi^2 EI}{4L^2} \quad (30)$$

Using Equation 29 the principal critical buckling load of cracked beam is determined. Throughout this study only elastic buckling is considered. The variations of the first non-dimensional buckling load (P_{cr}/P_e) of cracked beam with respect to different crack locations and ratios have been demonstrated in Figure 5. P_{cr} and P_e represent the principal buckling load of the cracked and intact beams, respectively. Cracks result in decreases in the critical buckling loads. Crack ratios and locations affect the buckling behaviour of the beam. A crack located in the section of maximum bending moments of the corresponding intact beam results in highest energy losses and consequently the largest reduction in the buckling loads. As expected, larger cracks situated near the fixed end of the beam produce higher drops in the buckling load, for instance, a relatively big crack (r/h = 0.8) near the fixed end (L_C/L = 0.1) reduces the fundamental buckling load about 80%. On the contrary, even it is comparatively big (r/h = 0.6), when a crack approaches to the free end it has little effects on the buckling load of the beam.

Vibration of axially loaded fixed-free beam with a crack

As previously presented, crack and applied compressive axial load decrease the overall stiffness of the beam, as a consequence the dynamical characteristics of the beam are modified. Free vibration of axially loaded cracked beam is completed by using equation 26. The results of the current study and those of Binici's (2005) are compared and as can be seen from Figure 6, very good conformities have been found between them. In the analysis, the crack ratio is taken to be r/h = 0.5. It is also apparent from Figure 6 that if the applied axial compressive load ratio gets higher, the frequency reductions also increase. Validation of the offered procedure gives the applicability of the method with confidence.

Axially loaded fixed-free beam with three cracks

Second sample is chosen as a fixed-free multi-cracked

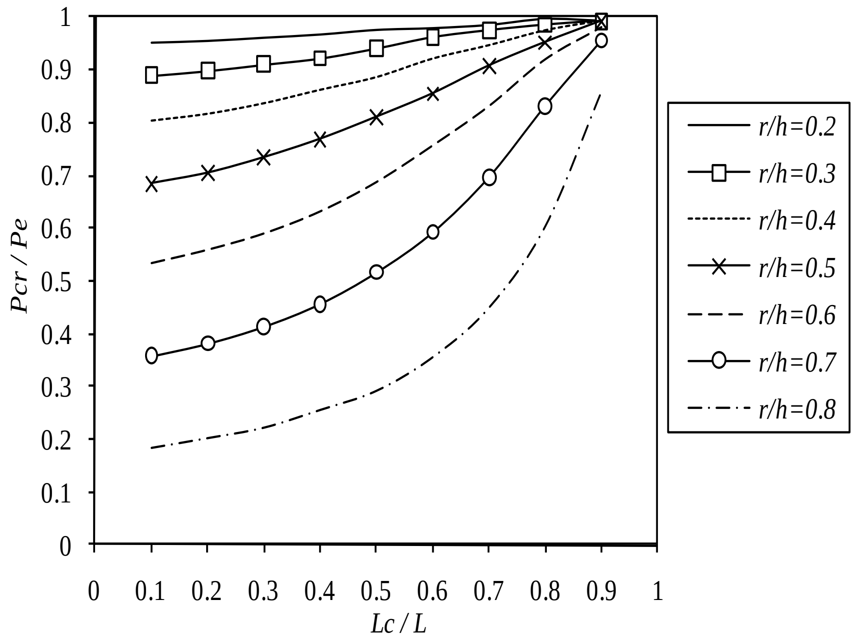

Figure 5. First non-dimensional buckling load of cracked beam with respect to different crack locations (*Lc/L*) and ratios (*r/h*).

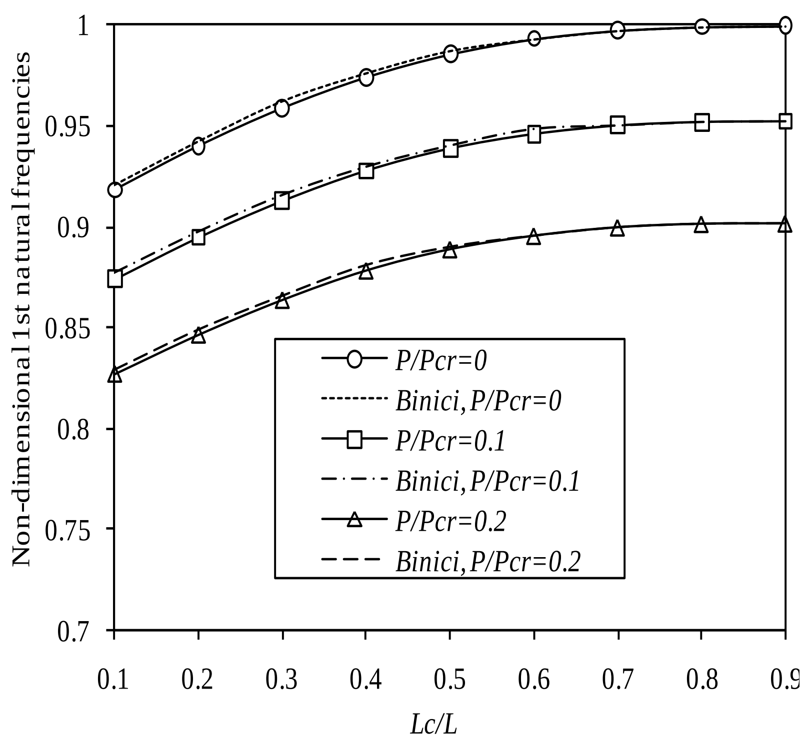

Figure 6. Literature comparison of first non-dimensional natural frequencies of axially loaded fixed-free cracked beam.

beam subjected to axial loading (Figure 7). The geometric and material properties of the beam in the current and subsequent cases are chosen as the same as they were in the previous case. It is clear that the load

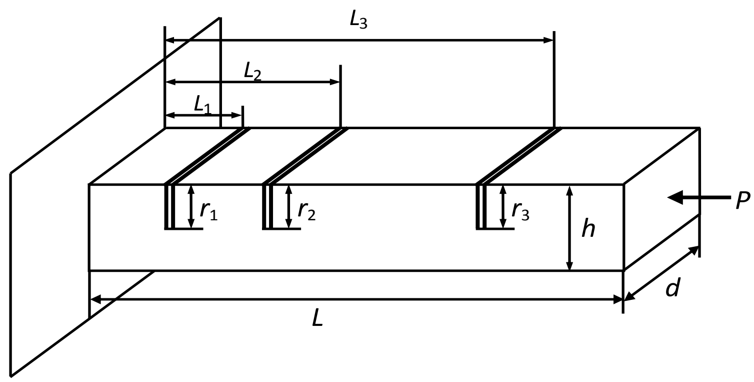

Figure 7. A fixed-free axially loaded beam with three cracks.

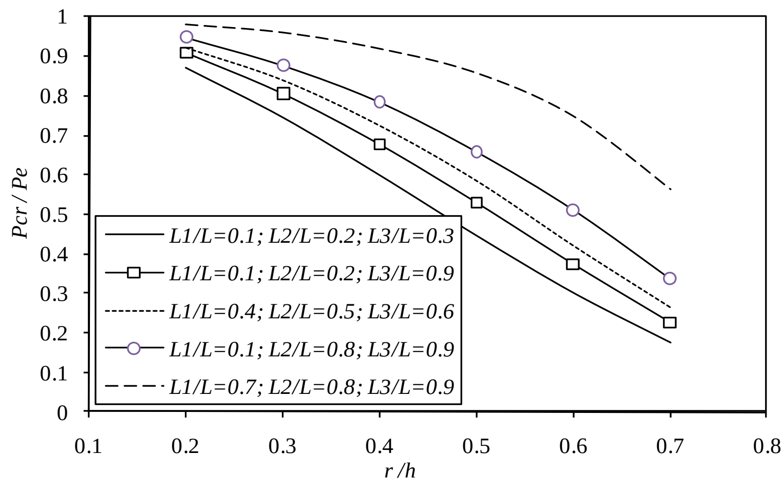

Figure 8. First non-dimensional buckling loads of multi cracked beam with respect to different crack locations and ratios.

applied to cracked beam should be less than the first critical buckling load, therefore similar to first case, as a first step a buckling analysis is carried out.

Buckling analysis of fixed-free beam with three cracks

The fundamental critical buckling loads of the fixed-free cracked and intact beams are found by using equations 29 and 30, respectively. Figure 8 illustrates the variation of the first non-dimensional buckling load (P_{cr}/P_e) of cracked and intact beam with respect to different crack locations and ratios. Cracks near the fixed end (L_1/L = 0.1, L_2/L = 0.2, L_3/L = 0.3), at the middle (L_1/L = 0.4, L_2/L = 0.5, L_3/L = 0.6) and near the free end (L_1/L = 0.7, L_2/L = 0.8, L_3/L = 0.9) with a crack ratio of r/h = 0.7 result in 83, 74 and 44% reduction in the first buckling load, respectively.

Vibration analysis of fixed-free beam with three cracks

Vibration analysis of fixed-free beam with three cracks under compressive axial loads P (P/P_{cr} = 0.05, P/P_{cr} = 0.15, P/P_{cr} = 0.25) is carried out by using Equation 26. The variation of the first, second and third non-dimensional natural frequencies (ω_{cr}/ω) of axially loaded fixed-free multi-cracked beam with respect to different applied axial loads (P/P_{cr}), crack locations (L_i/L) and crack ratios (r/h) have been given in Figure 9. It is observed from the figure that, crack locations, crack ratios and applied axial load levels strongly affect the natural frequencies of the beam. While the cracks near the fixed end cause more reductions in the first vnatural

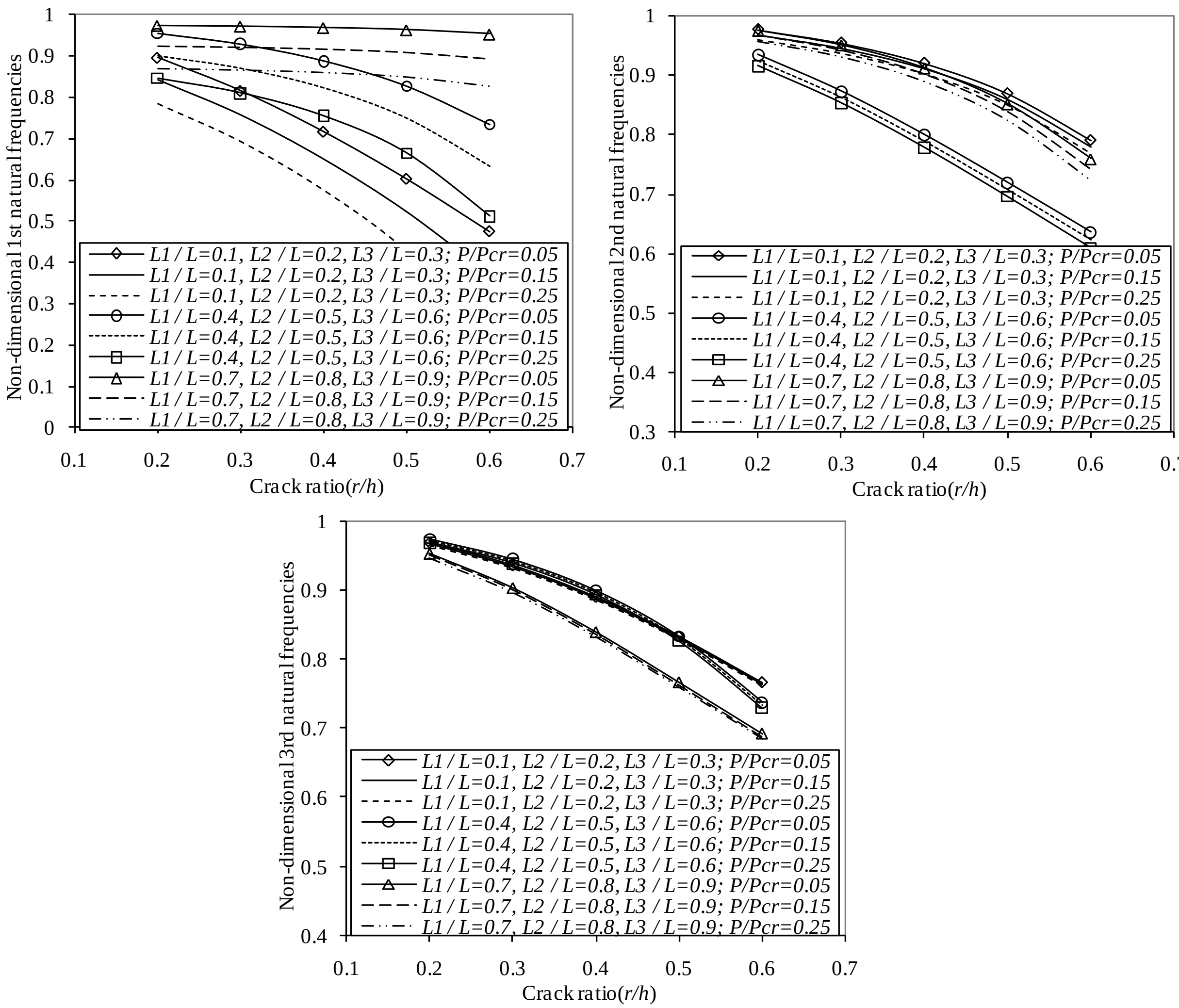

Figure 9. First, second and third non-dimensional natural frequencies of fixed-free multi cracked beam with respect to different applied axial loads, crack locations and crack ratios.

frequencies, second and third natural frequencies are most affected if the cracks are at the middle and near the free end, respectively. Figure shows that applied axial loads with the ratios of 5, 15 and 25% (P/P_{cr} = 0.05, 0.15 and 0.25) decrease the first natural frequencies of the fixed-free beam by 40, 48 and 58% compared to unloaded beam, respectively for crack locations L_1/L = 0.1, L_2/L = 0.2 and L_3/L = 0.3 with a crack ratio of r/h = 0.5. The same cracks result in reductions about 13, 14, 15% and 16, 17, 18% in the second and third natural frequencies for the applied axial load ratios of 5, 15 and 25% (P/P_{cr} = 0.05, 0.15 and 0.25), respectively.

The effects of cracks at different locations can be demonstrated from the figure. For a beam with three cracks (L_1/L = 0.4, L_2/L = 0.5, L_3/L = 0.6, r/h = 0.5), axial loads with the ratios of 5, 15 and 25% (P/P_{cr} = 0.05, 0.15 and 0.25) decrease the first natural frequencies about 17.5, 25 and 33.5%. Same cracks cause drops about 28, 29.5, 31% and 16.5, 17, 17.5% in the second and third natural frequencies for the applied axial loads of 5, 15 and 25% (P/P_{cr} = 0.05, 0.15 and 0.25), respectively. For the fixed-free beam, cracks (L_1/L = 0.7, L_2/L = 0.8, L_3/L = 0.9, r/h = 0.5) cause decreasing about 3.5, 9, 15%; 15, 16.5, 18% and 23.5, 24 and 24.5% in the first, second and third natural frequencies for the applied axial load ratios of 5, 15 and 25% (P/P_{cr} = 0.05, 0.15 and 0.25), respectively.

Deviation of the first, second and third mode shapes of the fixed-free beam with respect to different crack locations (L_1/L = 0.1, L_2/L = 0.2, L_3/L = 0.3; L_1/L = 0.4, L_2/L = 0.5, L_3/L = 0.6; L_1/L = 0.7, L_2/L = 0.8, L_3/L = 0.9), applied axial load ratios (P/P_{cr} = 0.05, 0.15, 0.25) and crack ratio r/h = 0.5 for the intact and loaded cracked beams are illustrated in Figures 10 to 12. From these figures it can be clearly seen that applied axial load ratios, crack locations and ratios play important role on

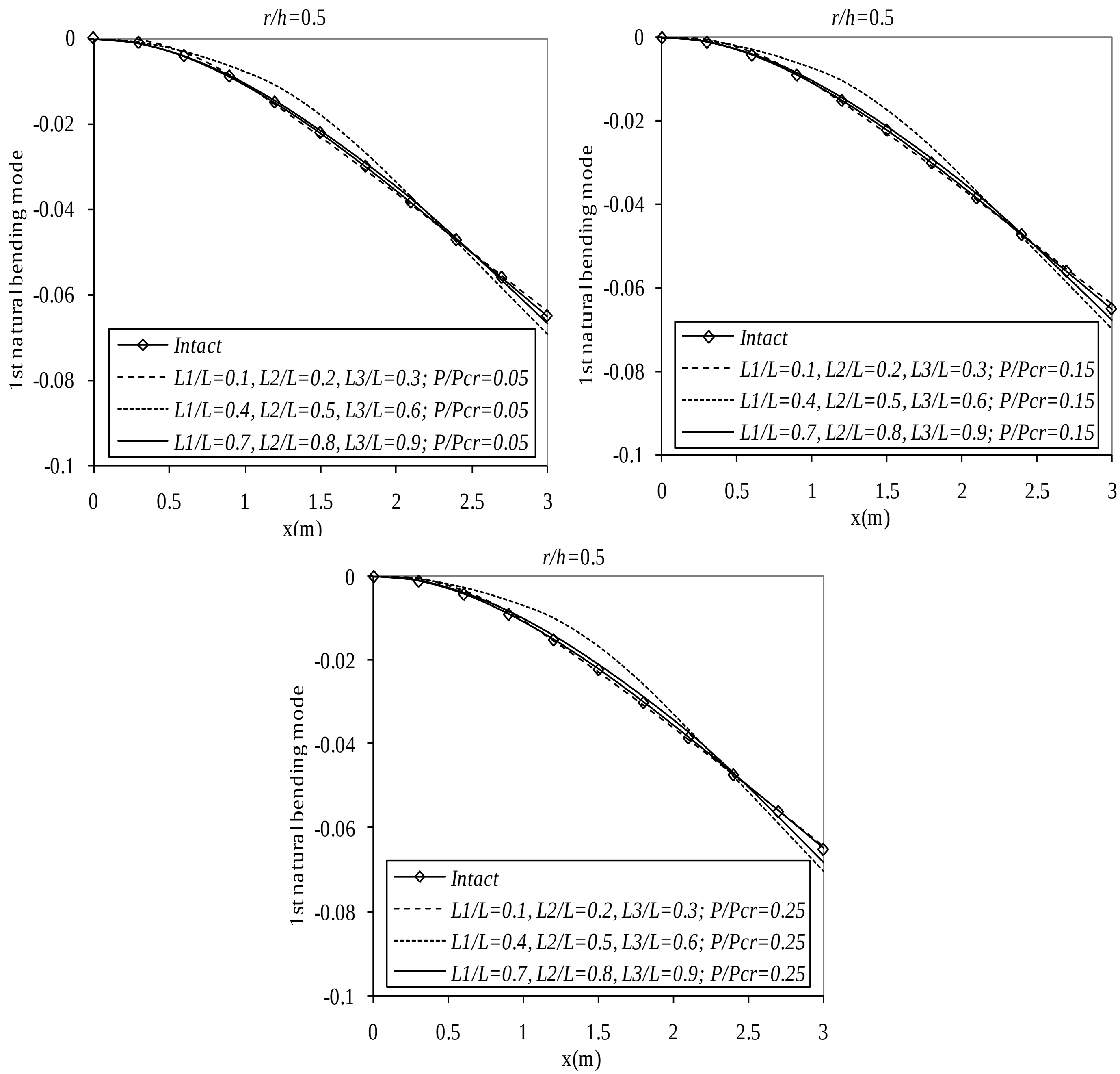

Figure 10. First mode shapes of fixed-free multi-cracked beam with respect to various applied axial loads, crack locations with the crack ratio of *r/h* = 0.5 for the intact and loaded cracked beams.

the variation of mode shapes. While the cracks located at certain locations have little effects in a particular mode shape and cannot be recognised, it is apparent from these figures that same cracks may have bigger effects on the other mode shapes and can be detected easily. As a consequence, all mode shapes should be checked for the crack detection process. This outcome is significant from the point of damage detection by means of mode shapes.

Axially loaded fixed-pinned double cracked beam

Buckling analysis of fixed-pinned double cracked beam

The third sample is a fixed-pinned double cracked beam subjected to axial loading (Figure 13). The fundamental critical buckling load of the fixed-pinned intact beam can be found by using the Euler Formula as:

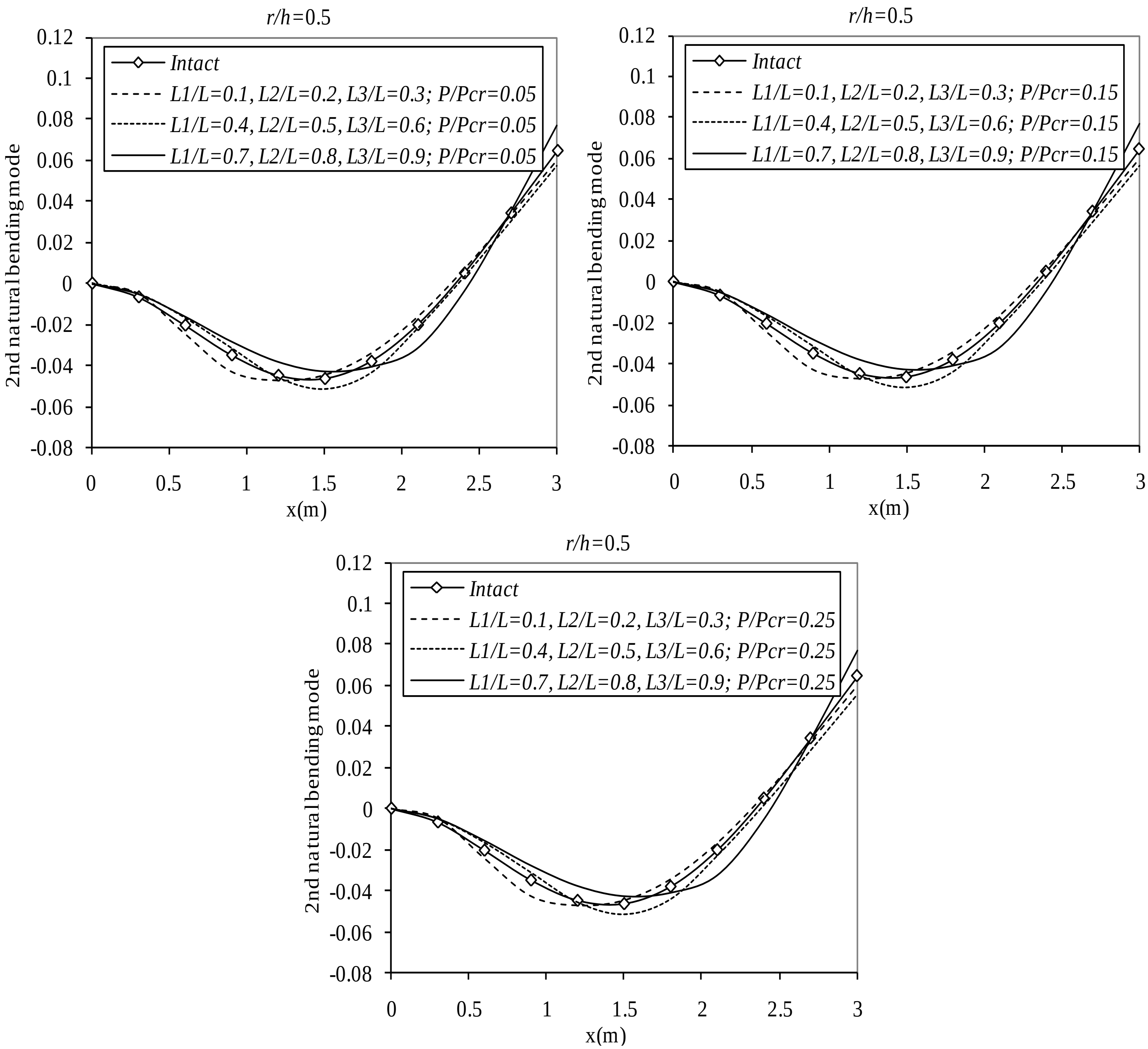

Figure 11. Second mode shapes of fixed-free multi-cracked beam with respect to various applied axial loads, crack locations with the crack ratio of *r/h* = 0.5 for the intact and loaded cracked beams.

$$P_e = \frac{\pi^2 EI}{(0.7L)^2} \quad (31)$$

Figure 14 illustrates the deviation of the first non-dimensional buckling load (P_{cr}/P_e) of cracked and intact beams with respect to different crack locations and ratios. If the cracks positioned near the 70 and 80% of the beam length (L_1/L = 0.7, L_2/L = 0.8) with a crack ratio of r/h = 0.7, 75% reduction in the first buckling load is observed. Quite the opposite, if the cracks are located near the inflection points (moment zero points of the corresponding intact beams) L_1/L = 0.2, L_2/L = 0.3 and quite big (r/h = 0.7) they have relatively little effect on the buckling load of the beam.

Vibration of axially loaded fixed-pinned double cracked beam

Using Equation 26 the vibration analysis of a fixed-pinned double cracked beam under axial loading is

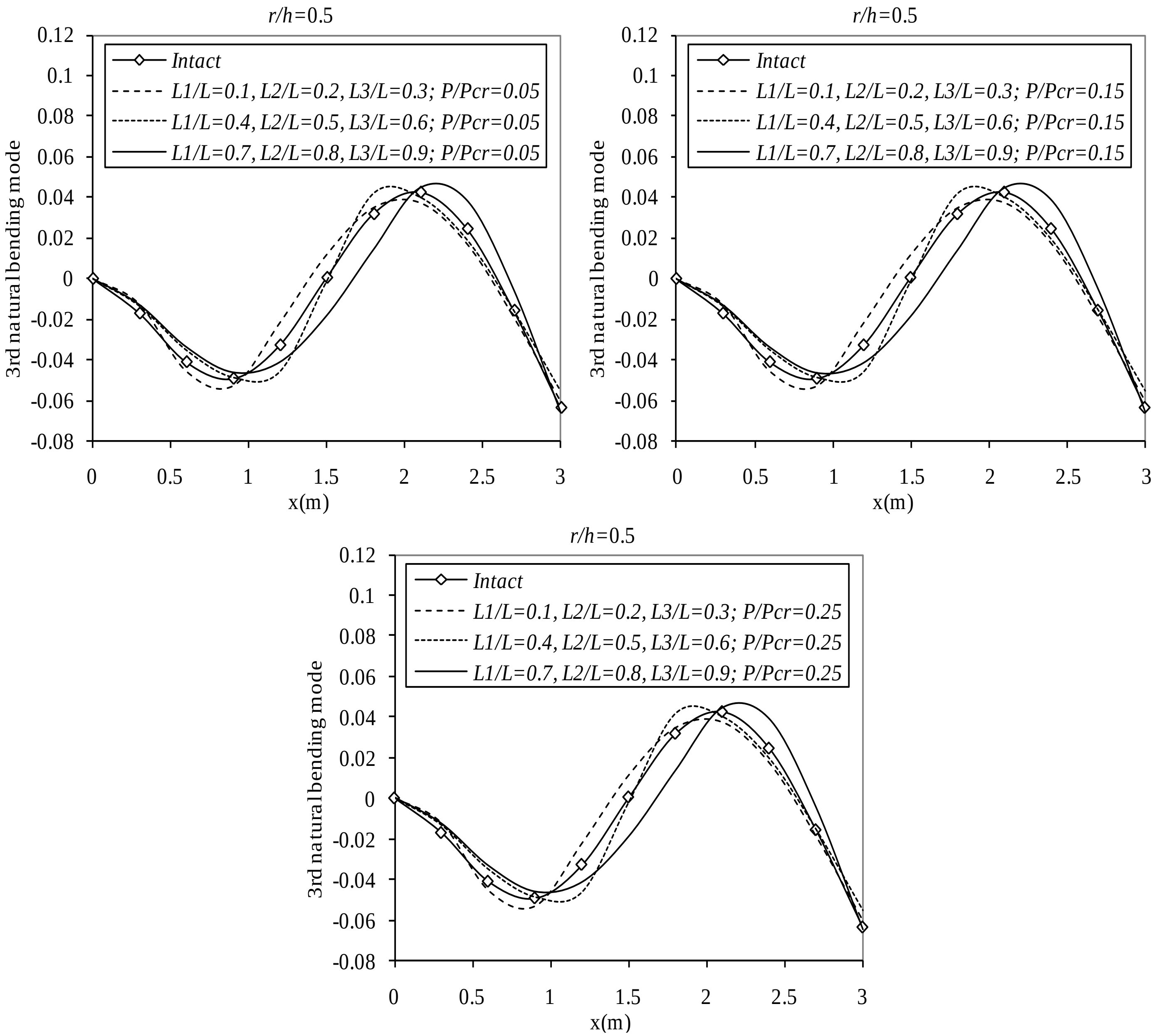

Figure 12. Third mode shapes of fixed-free multi-cracked beam with respect to various applied axial loads, crack locations with the crack ratio of r/h = 0.5 for the intact and loaded cracked beams.

completed. Figure 15 illustrates the deviation of the first, second and third non-dimensional natural frequencies of axially loaded fixed-pinned cracked beam with respect to different applied axial loads, crack locations and ratios. The cracks situated near the inflexion points (L_1/L = 0.2, L_2/L = 0.3) cause less effects on the first natural frequencies and relatively big changes in the second natural frequencies. On the other hand, cracks positioned by the middle of the beam (L_1/L = 0.5, L_2/L = 0.6) result in large reductions in the first and third natural frequencies. The figure shows that applied axial loads with the ratios of 5, 15 and 25% (P/P_{cr} = 0.05, 0.15 and 0.25) decrease the first natural frequencies of the fixed-pinned double cracked beam by 5, 11 and 17% compared to unloaded beam, respectively for crack locations L_1/L = 0.2, L_2/L = 0.3 and crack ratio r/h = 0.5. For different axial load ratios (P/P_{cr} = 0.05, 0.15 and 0.25), same cracks result in falls about 11, 13, 15% and 10, 11, 12% in the second and third natural frequencies, respectively.

The cracks at L_1/L = 0.5, L_2/L = 0.6 with the crack ratio of r/h = 0.5 cause the decrease of about 19, 26, 33%; 6, 8, 10% and 12, 13, 14% in the first, second and third natural frequencies for the applied axial load ratios of 5,

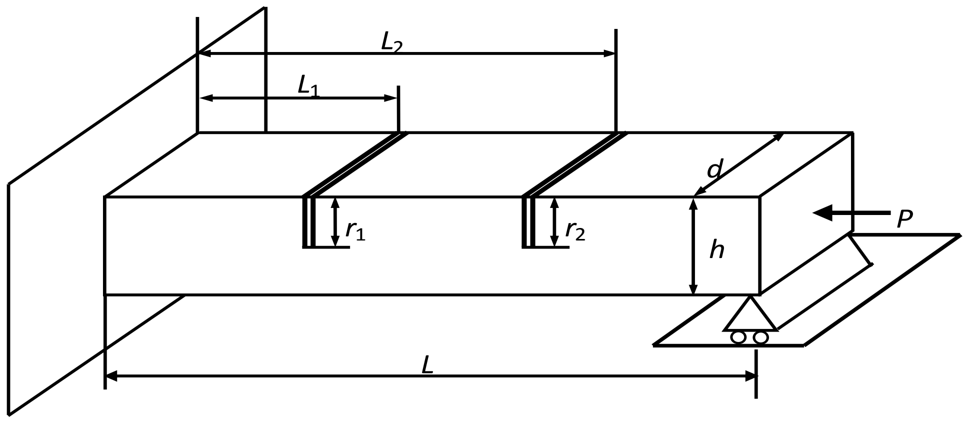

Figure 13. A fixed-pinned axially loaded beam with two cracks.

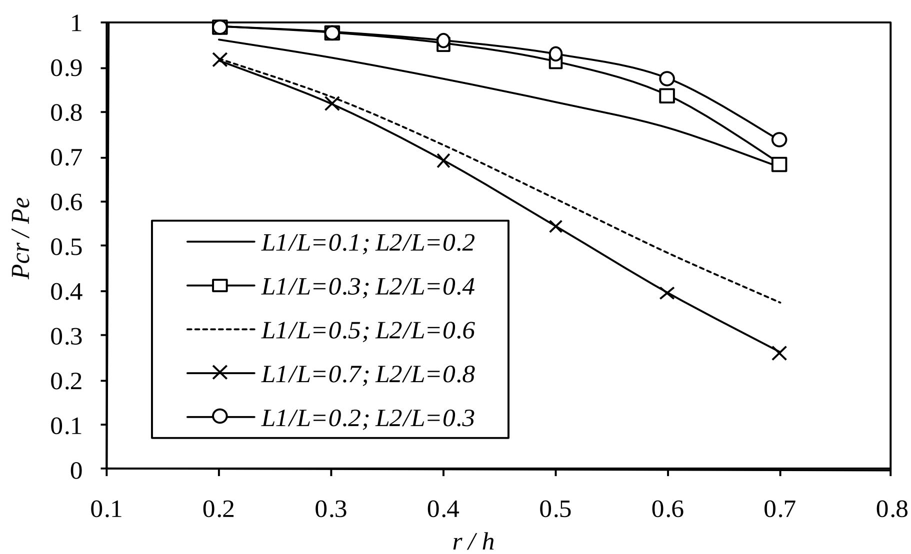

Figure 14. First non-dimensional buckling loads of double cracked beam with respect to different crack locations and ratios.

15 and 25% (P/P_{cr} = 0.05, 0.15 and 0.25), respectively. First, second and third mode shapes of the fixed-pinned double cracked beam with respect to crack locations L_1/L = 0.1, L_2/L = 0.2; L_1/L = 0.5, L_2/L = 0.5; L_1/L = 0.8, L_2/L = 0.9, applied axial load ratios (P/P_{cr} = 0.05, 0.15, 0.25) and crack ratio r/h = 0.5 for the intact and loaded cracked beams are shown in Figure 16. The positions of the cracks can be recognised from the mode shapes and this is more clearly perceived when the applied axial load ratio gets higher.

CONCLUSIONS

Vibration and stability analyses of multi-cracked beams under compressive axial load were numerically investigated by a new and efficient method utilising the component mode synthesis technique accompanied by the finite element method. The presented technique detaches a non-linear problem into linear components from the crack sections. The components were connected together by means of springs capable of carrying axial, shearing and bending effects. Ahead of the vibration analysis a buckling analysis was completed and critical buckling loads were found. Throughout the study only elastic buckling was considered and application of the current work is limited to the vibration and stability analyses of beams with non-propagating open edge cracks.

It was shown that crack ratios and locations affect the buckling behaviour of the beam. Big cracks have produced higher reductions in the buckling load, as

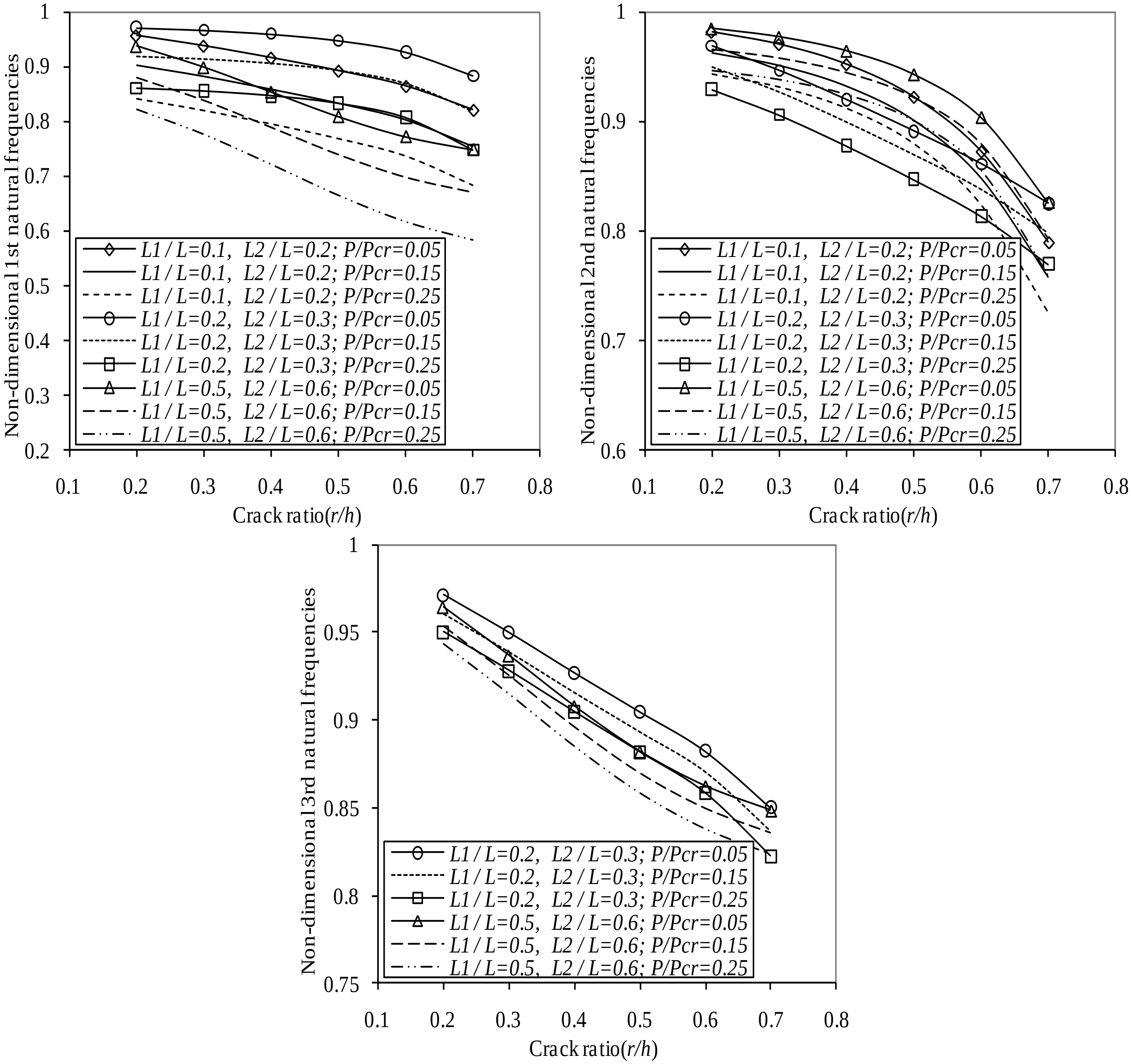

Figure 15. First, second and third non-dimensional natural frequencies of fixed-pinned double cracked beam with respect to different applied axial loads, crack locations and crack ratios.

expected. Applied compressive axial load levels, crack locations and ratios played important role on the variation of natural frequencies and mode shapes. Cracks and applied load decreased the overall stiffness of the beam and as a consequence, the dynamical characteristics of the beam were modified. Higher applied axial load ratios have produced more reductions in the natural frequencies and more changes in the mode shapes.

It was shown that the knowledge of modal data of cracked beams formed an important characteristic in assessing the structural failure. To reveal the efficiency of the procedure, results of the studied cases in the current work have been compared with earlier studies available in the literature leading to confidence in the validity of this approach. Presented numerical cases confirmed that the proposed method is effective for the vibration analysis of axially loaded multi cracked beams

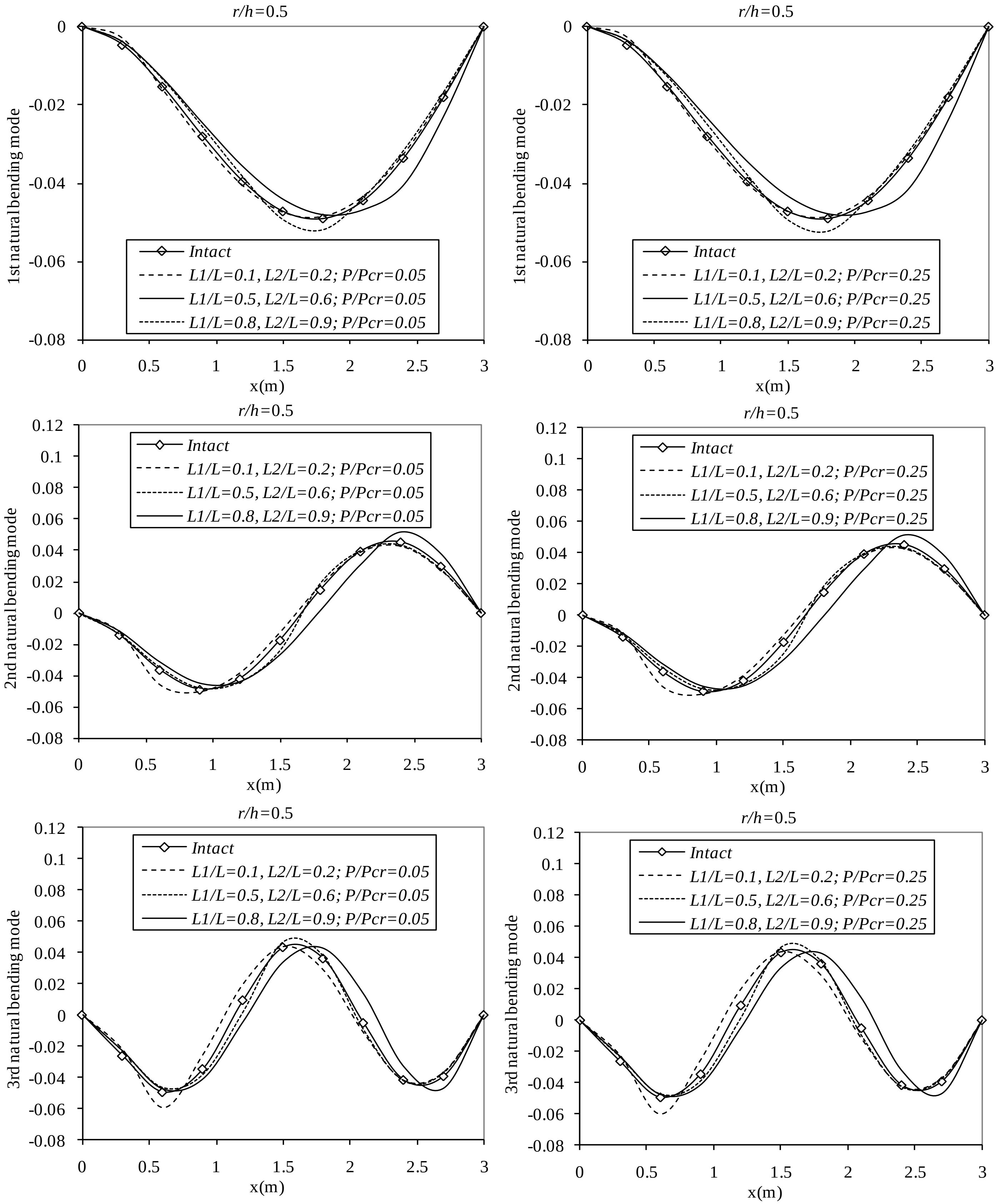

Figure 16. First, second and third mode shapes of fixed-pinned double cracked beam with respect to various applied axial loads, crack locations with the crack ratio of *r/h* = 0.5 for the intact and loaded cracked beams.

with any kind of end conditions.

Nomenclature: ***A*****,** Crack area; c_{ij}**,** flexibility coefficients; ***C*****,** flexibility matrix; ***d*****,** thickness of beam; D_i**,** damping matrix for component *i;* ***E*****,** Young's modulus of elasticity; $f_i(t)$**,** external force vector for component *i*; ***h*****,** height of beam; ***J*****,** strain energy release rate; K_i**,** stiffness matrix for component *i*; K_C**,** connection matrix; K_{cr}**,** stiffness matrix induced by crack; K_{Gi}**,** geometric stiffness matrix for component *i*; K_I**,** stress intensity factor for mode *I*; K_{II}**,** stress intensity factor for mode *II*; K_{III}**,** stress intensity factor for mode *III*; ***L*****,** length of beam; L_i/L**,** crack positions; M_i**,** mass matrix for component *i*; z_i**,** element numbers for component *i*; ***P*****,** applied compressive axial load; ***p, s*****,** principal coordinate vectors; P_{cr}**,** critical buckling load of cracked beam; P_e**,** critical buckling load of intact beam; ***q*****,** generalised displacement; r_i**,** crack length; r/h**,** crack depth ratio; ***T*****,** kinetic energy; ***U*****,** strain energy; ***u, v*****,** displacements with respect to *x* and *y* axes; θ**,** rotation about *z* axis; ψ**,** mass normalised modal matrix; ρ**,** material density; ϕ**,** modal matrix; ν**,** Poisson's ratio; ω**,** natural frequency; ω_{cr}**,** natural frequency of cracked beam.

REFERENCES

Arbodela-Monsalve LG, Zapata-Medina DG, Aristizabal-Ochoa JD (2007). Stability and natural frequencies of a weakened Timoshenko beam-column with generalized end conditions under constant axial load. J. Sound Vib., 307: 89-112.

Aristizabal-Ochoa JD (2007). Static and dynamic stability of uniform shear beam-columns under generalized boundary conditions. J. Sound. Vib., 307: 69-88.

Aydin K (2007). Vibratory characteristics of axially loaded Timoshenko beams with arbitrary number of cracks. J. Vib. Acoust., 129: 341-354.

Aydin K (2008). Vibratory characteristics of Euler-Bernoulli beams with an arbitrary number of cracks subjected to axial load. J. Vib. Control, 14: 485-510.

Bilgehan M (2011). Comparison of ANFIS and NN models-With a study in critical buckling load estimation. Appl. Soft Comput., 11: 3779-3791.

Binici B (2005). Vibration of Beams with multiple open cracks subjected to axial force. J. Sound Vib., 287: 277-295.

Caddemi S, Calio I (2009). Exact closed-form solution for the vibration modes of the Euler–Bernoulli beam with multiple open cracks. J. Sound Vib., 327: 473-489.

Cawley P, Adams RD (1979). The location of defects in structures from measurements of natural frequencies. J. Strain Anal. Eng., 14: 49-57.

Dimarogonas AD, Paipetis SA (1983). Analytical methods in rotor dynamics. Applied Science Publishers.

Friedman Z, Kosmatka JB (1993). An improved two-node Timoshenko beam finite element. Comput. Struct., 47: 473-481.

Gounaris G, Dimarogonas AD (1988). A finite element of a cracked prismatic beam for structural analysis. Comput. Struct., 28: 309-313.

Gurel MA (2007). Buckling of slender prismatic circular columns weakened by multiple edge cracks. Acta Mech., 188: 1-19.

Hsu MH (2005). Vibration analysis of edge-cracked beam on elastic foundation with axial loading using the differential quadrature method. Comput. Method. Appl. M., 194: 1-17.

Hurty WC (1965). Dynamic analysis of structures using substructure modes. AIAA J., 3: 678-685.

Irwin G (1960). Fracture mechanics, structural mechanics. Pergamon Press.

Kisa M (2004). Free Vibration analysis of a cantilever composite beam with multiple cracks. Compos. Sci. Technol., 64: 1391-1402.

Kisa M, Brandon JA (2000a). Free vibration analysis of multiple open-edge cracked beams by component mode synthesis. Struct. Eng. Mech., 10: 81-92.

Kisa M, Brandon JA (2000,b). The effects of closure of cracks on the dynamics of a cracked cantilever beam. J. Sound Vib., 238: 1-18.

Kisa M, Brandon JA, Topcu M (1998). Free vibration analysis of cracked beams by a combination of finite elements and component mode synthesis methods. Comput. Struct., 67: 215-223.

Krawczuk M (2002). Application of spectral beam finite element with a crack and iterative search technique for damage detection. Finite Elem. Anal. Des., 38: 537-548.

Krawczuk M, Ostachowicz WM (1993). Transverse natural vibrations of a cracked beam loaded with a constant axial force. J. Vib. Acoust., 115: 524-528.

Kukla S (2009). Free vibrations and stability of stepped columns with cracks. J. Sound Vib., 319: 1301-1311.

Lee S, Park T, Voyiadjis GZ (2002). Free vibration analysis of axially compressed laminated composite beam-columns with multiple delaminations. Compos. Part B-Eng., 33: 605–617.

Li QS (2001). Buckling of multi-step cracked columns with shear deformation. Eng. Struct., 23: 356–364.

Li QS (2003). Classes of exact solutions for buckling of multi-step non-uniform columns with an arbitrary number of cracks subjected to concentrated and distributed axial loads. Int. J. Eng. Sci., 41: 569–586.

Mei C, Karpenko Y, Moody S, Allen D (2006). Analytical approach to free and forced vibrations of axially loaded cracked Timoshenko beams. J. Sound Vib., 291: 1041-1060.

Patil DP, Maiti SK (2003). Detection of multiple cracks using frequency measurements. Eng. Fract. Mech., 70: 553-572.

Ruotolo R, Surace C, Crespo P, Storer D (1996). Harmonic analysis of the vibrations of a cantilevered beam with a closing crack. Comput. Struct., 61: 1057-1074.

Shen MHH, Chu YC (1992). Vibrations of beams with a fatigue crack. Comput. Struct., 45: 79-93.

Shifrin EI, Ruotolo R (1999). Natural frequencies of a beam with an arbitrary number of cracks. J. Sound Vib., 223: 409-423.

Takahashi I (1998). Vibration and stability of a cracked shaft simultaneously subjected to a follower force with an axial force. Int. J. Solids Struct., 35: 3071-3080.

Viola E, Federici L, Nobie L (2001). Detection of crack location using cracked beam element method for structural analysis. Theor. Appl. Fract. Mech., 36: 23-35.

Viola E, Ricci P, Aliabadi MH (2007). Free vibration analysis of axially loaded cracked Timoshenko beam structures using the dynamic stiffness method. J. Sound Vib., 304: 124-153.

Wang Q (2004). A comprehensive stability analysis of a cracked beam subjected to follower compression. Int. J. Solids Struct., 41: 4875-4888.

Yang J, Chen Y, Xiang Y, Jia XL (2008). Free and forced vibration of cracked inhomogeneous beams under an axial force and a moving load. J. Sound Vib., 312: 166-181.

Zheng DY, Fan SC (2003). Vibration and stability of cracked hollow-sectional beams. J. Sound Vib., 267: 933-954.